Simple Data-Driven Modeling of Brushes

William Baxter[*]
Microsoft Research

Naga Govindaraju[†]
Microsoft Research

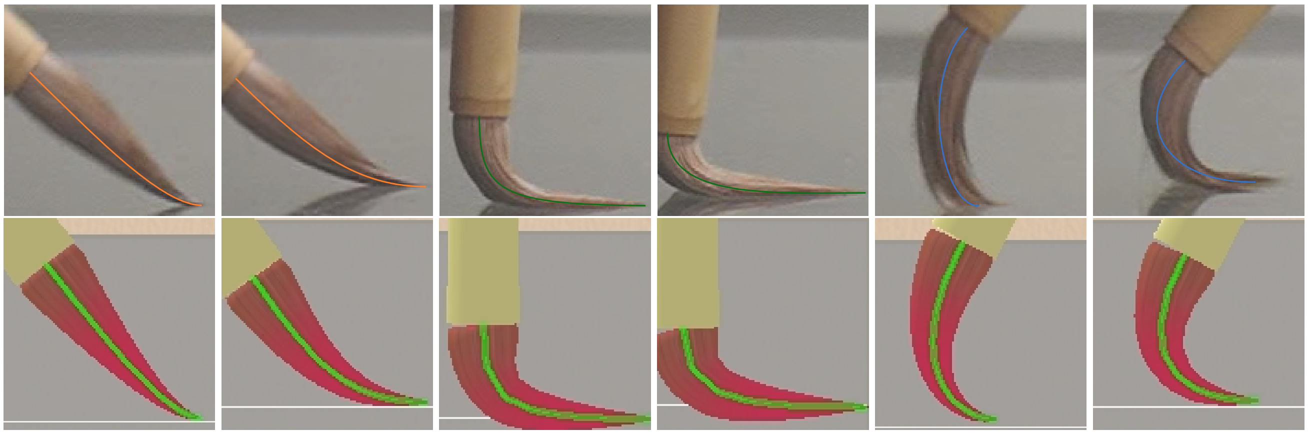

Figure 1: *We create a dynamic deformable 3D brush based on measurements taken of actual brush deformations (top row). A small table of such measurements (see Figure 3) is enough to recreate the key deformation characteristics of a brush (bottom row), and the result is a fast, stable and realistic brush model for use in a digital painting system.*

Abstract

We present a new and simple data-driven technique for modeling 3D brushes for use in realistic painting programs. Our technique simplifies and accelerates simulation of the constrained dynamics of brushes by using a small lookup table that efficiently encodes the range of feasible constrained states. The result is a brush model which runs an order of magnitude faster than previous physics-based methods, while at the same time delivering greater deformation fidelity.

Keywords: deformation, painting systems, data-driven, example-based, dynamics, optimization, physically based modeling

1 Introduction

Physically-realistic virtual brushes enrich a painting system by giving digital paint a dynamic expressiveness closer to that of real-world paint. In a typical stamp-based digital painting program, the range of marks each brush bitmap can generate is limited. Most programs offer at most a simple scaling of these bitmaps based on pressure. To overcome the lack of realistic brush dynamics, these programs typically provide hundreds of pre-made brush bitmaps with many different shapes. The result is that changing brushes becomes a time-consuming activity for the user. In contrast, the dynamic nature of real-world, physical brushes allows painters to quickly create a rich variety of different marks with each single brush, depending upon how they wield and load it. Importantly, this flexibility does not incur a high cognitive load, thanks to the intuitive familiarity of physical deformations.

A good physically-based brush model can give the digital artist nearly the same level of flexibility and intuitive control as can be had with brushes in the physical world. The previously proposed brush models that offered this level of physical accuracy have all relied upon simulation using costly numerical techniques. Though these techniques can run at interactive frame rates, for a painting system, frame rate is not as important as the impression rate. Impression rate is the number of brush impressions which can be stamped per second. The ideal impression rate is several orders of magnitude higher than the frame rate—6000 Hz or more is desirable to prevent lag on fast stroke motions. The necessary impression rate is determined by the speed of the brush in pixels/sec, so the exact rate required depends on both the DPI of the canvas being drawn upon, and the speed with which the user is drawing.

As many cycles as possible are needed for generating impressions. If the stroke engine lacks the time to generate the impressions required for a stroke, either the display will lag behind input, or strokes become tessellated as input samples are dropped without updating the brush deformation. Current physical brush simulations can require a millisecond or more to simulate a brush head with several bristles, taking valuable cycles away from impression generation.

A further difficulty with purely simulation-based approaches is matching the behavior of specific real-world brushes. Real brushes have a stiffness that varies from tip to belly, which can be difficult to match convincingly by setting a handful of stiffness parameters.

Subtle deformations near the tip, the most pliable part of the brush, are also difficult to recreate accurately using a model that is discretized as coarsely as is typical with previous approaches. Finer discretization has not been possible due to performance and numerical issues.

We present a new data-driven technique for simulating brushes

[*]e-mail: wibaxt@microsoft.com
[†]e-mail:nagag@microsoft.com

based on real, measured brush deformations that offers a solution to these limitations. Our technique is an order of magnitude faster than previous simulation approaches while more accurately modeling subtle tip deformations. And since our technique is data-driven, it is simple to match the deformation behavior of specific brushes with significantly less parameter tweaking.

2 Previous Work

Brush modeling has been very well-studied in the digital painting literature. In this section, we briefly review these techniques, as well as some techniques for non-brush modeling using data.

Non-physics 2D brushes: The earliest and still most commonly used model for brushes are those based on a simple 2D bitmap, stamped repeatedly along a user's stroke [Photoshop 2009; ArtRage 2009; Painter 11 2009; Smith 1978; Strassmann 1986]. These techniques may apply some simple transformations to the bitmap while stamping the footprint along the stroke. 2D techniques are fast but less flexible than real 3D brushes.

Non-physics 3D brushes: In these techniques, a collection of parameters are used to model 3D brush strokes [Wong and Ip 2000; Xu et al. 2002; Xu et al. 2003]. These techniques improve the flexibility in modeling complex strokes as compared to non-physics 2D brushes but may require significant effort in capturing the model parameters to create realistic brush strokes.

Dynamic 3D brushes: Baxter et al. [2001] modeled the brush dynamics using a semi-implicit technique that integrates linear springs between the brush head and the canvas. Adams et al. [2004] later improved this technique by using a leap-frog integration scheme. The use of time-stepping integration techniques may not be suitable for simulating stiff bristles.

Optimization-based 3D brushes: Saito et al. [Saito and Nakajima 1999] approximate the bristle behavior using a quasi-static energy optimization technique on a single spine. Chu and Tai[2002] incorporated lateral spine nodes to allow brush flattening. Baxter et al. [2004] later used a similar optimization technique, adding multiple spines and subdivision surfaces to model a wider variety of brush geometries. These techniques are relatively expensive and may require significant engineering, and exhaustive parameter tweaking to generate realistic behavior.

Data-based brushes: In order to model visual effects from traditional tools and media, Greene [Greene 1985] introduced the drawing prism to capture the images of tool movement on the surface. Peter Vandoren et al.[2009] updated this idea with novel capture hardware and used the footprints captured from real wet brushes. These techniques have an advantage of providing an intuitive haptic feedback of a real brush and can capture complex brush strokes. However, a user must actually possess the full range of sizes and shapes of physical brushes she would like to use. Furthermore, it is non-trivial to incorporate both forward and backward paint transfer between the canvas and the brush.

Data-driven simulation: Data-driven techniques have been used in other areas of simulation, for instance in animating cloth [Cordier and Magnenat-Thalmann 2004; White et al. 2007]. Though in many ways more general than the technique we present, these techniques are not particularly suited to the task of simulating brushes in real time.

3 Table-driven simulation

Like many previous works [Saito and Nakajima 1999; Chu and Tai 2002; Baxter and Lin 2004; Van Laerhoven and Reeth 2007], our model uses a set of control bristles or spines to guide the deformation. This keeps the amount of required computation to a minimum. The control bristles are simulated, while the remaining brush geometry is deformed kinematically based on the motion of the control bristles.

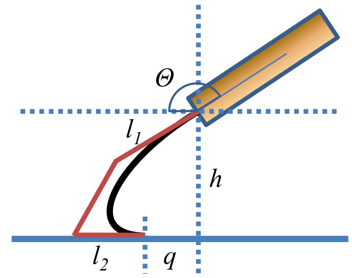

Figure 2: *The geometry of a reference deformation of a control bristle. Triplets (l_1, l_2, q) are indexed in the deformation table by the bristle base angle, θ, and handle height, h. l_1 and l_2 are the lengths of the sides of first and last edge of the cubic Bézier control polygon.*

The main observation motivating our approach is that typical deformations of a brush can be described succinctly as a set of simple curves. Previous approaches have used costly iterative constrained optimization techniques to find the minimum energy state of each control bristle [Saito and Nakajima 1999; Chu and Tai 2002; Baxter and Lin 2004; Van Laerhoven and Reeth 2007]. But we observe that, ultimately, the space of minimal energy configurations of a bristle is in practice fairly low-dimensional.

3.1 Creating the Deformation Table

Typical bristle deformations lie on or near a plane. This observation enables us to make a dramatic simplification to our model. Instead of capturing 3D deformations we may just capture deformations in a single reference plane. This leads to a parametrized space of deformations with just two degrees of freedom. We take the first to be the height of the bristle root over the canvas surface, and the second to be the angle of attack at the root of the bristle (see Figure 2).

3.2 Equilibrium bend energy

These curves give a record of the static bend energy equilibria configurations of the brush. They in essence encode solutions to the engineering problem of a simply supported non-linear beam with one clamped end. Such solutions ignore friction and just tell us about static equilibria of the bending energies.

Several of these deformations for a particular brush, and our reconstructed deformations for these are shown in Figure 1. The full table of deformation curves constructed for the brush is shown in Figure 3.

For now we simply trace these curves out by hand in a vector drawing program, following the centerline of the deformed brush in frames extracted from a video. We found that each deformation could be adequately modeled as a single cubic Bézier segment, though accuracy may be slightly improved using a fourth order curve. In principle this curve extraction process could be automated using image segmentation and optimal fitting of curves to the medial axis.

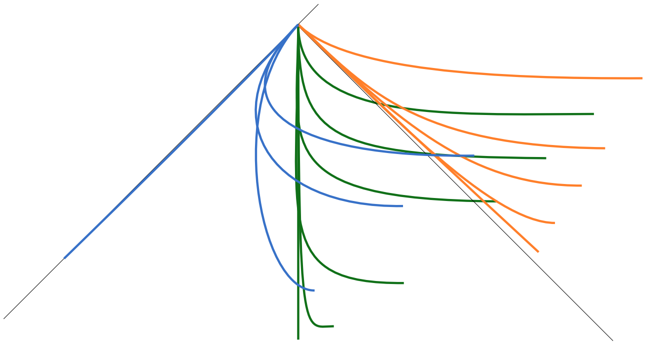

Figure 3: *The complete table of deformation curves for the round calligraphy brush in Figure 1. The colors correspond to different angles of the brush handle with respect to the canvas surface.*

In the remainder of the paper, we assume a rest pose coordinate system for the brush in which the canvas is the X-Y plane and the brush handle, in its rest pose, points up along the +Z direction. Reference deformations are assumed to be in the X-Z plane.

In storing the table, we can make several optimizations. The directions of the tangents at the ends of the curves are predetermined by the ferrule on one end, and the canvas, which acts as the simple support at the other. So in practice we only need to store the lengths of these tangents, not their directions. We translate each curve root to the origin, so the only remaining data to store is the location of the distal control point on the curve. However the Z coordinate is just the height of the bristle, which is a lookup parameter, so only the X coordinate needs to be stored. Thus each curve entry can be stored using just 3 floating point values, two tangent lengths and the X coordinate of the bristle's tip.

To find the equilibrium bend energy curve using the table, we approximate with a bilinear interpolation using the four closest data points in terms of angle, θ, and a normalized height, $\hat{h}$. This normalized height is 1 at the point the bristle is just in contact with the surface, and 0 when the bristle root reaches the canvas. This allows the heights at different angles to be meaningfully interpolated. The result of the lookup is the end tangent lengths and the X position for the distal control point (l_1, l_2, and q in Figure 2).

The basic idea is to then rotate this curve in the reference X-Z plane to coincide with the equilibrium bend energy plane. This equilibrium plane is the plane perpendicular to the canvas, and passing through the transformed bristle root's tangent (the one with length l_1.) See Figure 2. This can be accomplished by applying an appropriate rotation about the Z axis to each of the reference control points.

There is one complication, however, in that for each given bristle angle there are two possible equilibrium positions corresponding to bristles bent forward and bristles bent backwards. We disambiguate these two cases by looking up both angles (α and $\pi - \alpha$) and picking the one that puts the brush tip closest to the place where it was in the previous frame.

3.3 Friction

The table of equilibrium energy states basically encodes the configuration that the brush would take if all friction were neglected. In order to give the brush more realistic dynamic behavior, it is necessary to incorporate friction into the model as well.

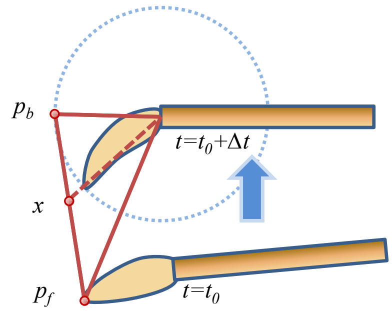

Figure 4: *A simplified energy optimization procedure incorporates bend spring and friction terms to determine the updated direction for the brush tip, x.*

Frictional forces act to keep the status quo. Thus ignoring spring energy, a bristle would tend not to move from frame to frame. So in some sense the optimal configuration with respect to friction is simply the previous configuration. This gives us two reference configurations: the bend energy equilibrium configuration from the previous section, and this friction-only configuration.

As in [Baxter and Lin 2004], by assuming that within a given time step points move linearly, we can treat friction as a cone-shaped energy well which requires work to escape. This follows from the Coulomb model of friction which offers a constant resistive force in the opposite direction of any motion. Integrating this leads to the cone-shaped well. The energy required to move from p_f to position x is thus:

$$E_f = \mu f_N \|p_f - x\|,$$

where μ is a coefficient of friction, f_N is a normal force, p_f is the position a point had last step, and x is the unknown equilibrium position for which we wish to solve (see Figure 4).

Bending energies on the other hand tend to be well approximated by quadratic functions in bend angles:

$$E_b = k_b |\phi|^2,$$

where k_b is a bending spring constant, and ϕ is the bend angle of a particular joint of a discretized control bristle. In [Chu and Tai 2002; Baxter and Lin 2004; Van Laerhoven and Reeth 2007], these relations are summed up joint-wise in 3D to get a total energy function and then solved for using non-linear optimization. However, ultimately, motions of different joints and the bend angles between them are highly correlated because the quadratic energy penalizes outliers. Neighboring joints tend to have similar ϕ.

So our approach is to just look at one representative point, the tip of the control bristle, and instead of looking at bend energy as a function of bend angle, we use the small angle approximation to arrive at:

$$E_b = k_b \|p_b - x\|^2,$$

where p_b is the bend energy equilibrium position that bristle tip would attain if friction were ignored. Note that we already account for the bending energy due to the canvas constraint in our lookup table, thus for our purposes this k_b represents only lateral bending in the X-Y plane. Summing E_f and E_b together it can be shown that the minimum energy solution must lie on the line between p_f and p_b. This allows us to reduce the problem to one dimension, and this can be solved analytically.

The minimum is at $x = p_f + \xi(p_b - p_f)$ where ξ is

$$\xi = \max\left(0, \frac{k_b\|p_b - p_f\| - \mu f_N}{k_b\|p_b - p_f\|}\right)$$

In our experiments we found $k_b = 1$ and $\mu = 0.75$ to work well with $f_N = 1$. We also tried adding a normal force based on the brush compression ratio, κ. For this case we use $f_N = 0.7 + 20 * \kappa^2$, with $\mu = 0.2$ and $k_b = \kappa$.

Once the minimum value for x is found, we actually use this as the direction in which to orient the third and fourth control points of the Bézier, while the second control point still uses the the p_b direction explained previously. This effectively models how friction pulls on the tip of the brush, but does not change the tangent of the end of the bristle that is clamped by the brush's ferrule.

We do not currently model internal brush friction explicitly, though it could be considered as being lumped in as part of the single friction energy.

3.4 Mesh deformation and skinning

For mesh deformation based upon the motion of the control bristles, we first subdivide each Bézier curve non-uniformly in unit arclength at points s_o according to the following cubic function:

$$s_o = \frac{1}{2}s^3 - \frac{3}{2}s^2 + 2s$$

where $s = i/n$ for $i = 0 \ldots n$. The non-uniform spacing has the effect of placing more points near the tip where higher curvature deformations are expected. A great benefit of our technique is that the overall cost is linear in the number of segments, with a small constant, whereas adding more segments in previously presented 2nd-order optimization methods grows as $O(n^3)$ due to linear systems that must be solved in the inner loop. A comparison of timings can be found in Figure 6.

To actually deform mesh vertices we use standard linear blend skinning (LBS), which allows us to use fast hardware-based vertex shaders to implement the deformation. Since standard LBS is a general spatial deformation technique, as with the FFD method of [Van Laerhoven and Reeth 2007], the brush geometry need not be a closed mesh or even a mesh. Any vertex-sampled geometry can be deformed, as can be seen in Figure 8.

3.4.1 Vertex weight assignment

To assign bone weights to vertices, we first used the equilibrium heat diffusion method of [Baran and Popović 2007], but found this method ultimately unsuitable for our application. The main issues were 1) it assumes a well-connected mesh (so it is not suitable for a triangle soup) 2) heat sources are set up by adding a source term for the closest bone to each vertex. This means if a bone is not the closest bone for any vertices it will have no influence at all. 3) the method seems best at creating tightly localized blending regions, rather than smooth gradual transitions – good for actual rigid skeletons, but not for our problem of smooth surface reconstruction from a discrete set of nonrigid frames. This last property is probably due to the lack of smoothness of harmonic solutions near constraints.

Instead we use a technique based on radial basis functions (RBF). We use the kernel function $\Phi(x, y) = \|x - y\|$ which corresponds to a bi-Laplacian fit to the data in 3D [Wahba 1990], and yields smoother results than a harmonic, or Laplacian, solution.

We determine a set of RBF coefficients $\mathbf{C}_{ij}$ by solving the linear system:

$$\mathbf{\Phi C} = \mathbf{F} \tag{1}$$

Where $\mathbf{\Phi}_{ij} = \Phi(x_i, x_j)$. The sites x_i, $1 \le i \le N_{\text{sites}}$, are determined by sampling each bone along its length (we choose 5 samples per bone). The right-hand-side data terms are defined as:

$$\mathbf{F}_{ij} = \begin{cases} 1 & \text{if point } x_i \text{ on bone } j \\ 0 & \text{otherwise} \end{cases} \tag{2}$$

From this we determine provisional vertex weights $\tilde{w}_{jk}$ with $1 \le j \le N_{\text{bones}}$ and $1 \le k \le N_{\text{vertices}}$ according to the RBF formula:

$$\tilde{w}_{jk} = \sum_{i=1}^{N_{\text{sites}}} \mathbf{C}_{ij} \Phi(x_k, x_i) \tag{3}$$

These are essentially a set of N_{bone} smooth cardinal functions each with a value of 1 on the given bone 0 on other bones. For the final weights, w_{jk}, we drop all but the four largest weights at each vertex and re-normalize. The restriction to the four most influential bones is a performance optimization that allows more efficient skinning with hardware vertex shaders.

Note that this weight truncation could lead to visible discontinuities, though in practice we have not observed any. If they did appear they could be eliminated by adding extra sites with $\mathbf{F}_{ij} = 0$ to the RBF interpolation. This would work as follows. For each bone we can associate a sort of 4th-order Voronoi region representing the zone in which that bone is one of the four closest bones. All vertices outside this region can be added as zero-valued sites relative to the given bone. In this way we could approximately enforce that there be no more than four influential bones per vertex while still obtaining a smooth RBF interpolation function. The down side would be a much larger linear system to solve. We have not observed a need for this technique so we have not implemented it at this point.

3.4.2 Matrix determination

As a brush is deforming, we must determine at each step what transformation matrix to associate with each bone. A simple but incorrect approach is to just take the matrix with uniform scale that rotates a bone in its rest configuration $[p_0, p_1]$ to the bone in its deformed position $[q_0, q_1]$, by rotating about the axis $(p_1 - p_0) \times (q_1 - q_0)$. This possible for a single-spine brush, but we wish to have a more general technique which can be applied to brushes with any number of spines. Given several spines, we wish to infer an optimal transformation to associate with each bone, based on the relative configurations of all the other spines. If bristles spread apart in one direction, the matrices need to reflect that directional scaling.

Our basic idea is to use a constrained least-squares fit to the guide bristles to find each segment's optimal matrix. Recently, many works such as [Müller et al. 2005; Rivers and James 2007] have used a least-squares technique where an orthogonality, or rigidity constraint is applied. In our case we know that bristles are inextensible along their length, but tufts of bristles may behave non-rigidly in orthogonal directions.

The inextensibility constraint is simply that the segment $[p_0, p_1]$ must be transformed into $[q_0, q_1]$. Subject to this constraint we wish to minimize a weighted least-squares estimate of the local transform. If p_i are sample points on bones in their rest pose and q_i are the corresponding points in the deformed configuration, we can solve the problems:

$$A_j = \underset{A}{\operatorname{argmin}} \sum_{i=1}^{N_{\text{samples}}} \eta_i \|A(p_i - p_j) - (q_i - q_j)\|^2$$

for all $1 \le j \le N_{\text{bones}}$ subject to the constraint. The points p_j are chosen as the midpoint of each bone, and p_i are the endpoints of the bones. We enforce the constraint approximately using a large penalty weight ($\eta_i = 500$) for any points p_i which are endpoints of the segment of p_j.

For other points we use an approximate inverse square law for the weighting, $\eta_i = 1/(d^2 + 0.1)$. However, since the scaling in the bristle direction is determined by our constraint, we should give higher weighting to points located along other directions. We make X-Y distances the dominant factor in the weights by defining $d = \sqrt{\Delta x^2/100 + \Delta y^2/100 + \Delta z^2}$.

Solving the final least squares problem requires care because for many brush geometries the problem is underdetermined. For instance if there is a single spine or all spines lie in a plane, then the appropriate off-axis or off-plane scale cannot be determined. Thus we solve using a singular value decomposition of the normal matrix $U\Sigma V^T = PEP^T$ (where P is formed by concatenating the p_i together column-wise, and E is a diagonal matrix with $E_{ii} = \eta_i$).

In non-degenerate cases where all singular values in Σ are non-zero, the solution is standard, just $R_{\text{fit}} = V\Sigma^* U^T QEP^T$, where

$$\Sigma^*_{ii} = \begin{cases} 1/\Sigma_{ii} & \text{if } \Sigma_{ii} \neq 0 \\ 0 & \text{otherwise.} \end{cases}$$

For degenerate cases with some zero singular values, we need to substitute a default scaling to complete the missing information in the result matrix. Post-multiplication of R_{fit} by U rotates the null axes into the last columns, where we set them to be perpendicular to the non-degenerate axes, with default scaling. For the case of one missing axis we use the geometric mean of the two existing axes scales. A final post-multiplication by U^T gives us the final R_{fit}.

For single spine brushes, a simpler approach is possible. There, for each segment, the associated transform is computed as the concatenation $R_{\text{bend}} R_{\text{twist}}$, where R_{bend} is the matrix that rotates the bristle base to the proper bend angle and R_{twist} is the rotation of the bristle base about the Z-axis.

3.5 Tip spreading

Like [Chu and Tai 2002] we have also added an explicit term to control tip spreading for certain brushes. In our formulation the fraction of tip spreading, t_{spread} is controlled by two factors. First, the previously mentioned compression ratio, κ. Second is the bend angle θ used in the table lookup. We use

$$t_{\text{spread}} = \text{smoothstep}(0, \frac{1}{2}, \kappa)\text{smoothstep}(\frac{\pi}{4}, \frac{\pi}{2}, \theta),$$

where *smoothstep* is the standard Hermite function. This effectively increases spreading for higher pressure and steep angles of attack. See Figure 5 for further details on the calculation of the spread factor for each vertex. The maximum spread ratio is a brush modeling parameter, which we denote k. A spread of $1 + t_{\text{spread}}(k-1)$ is attained at the tip of the brush. The base of the brush has a constant spread factor of 1. The spreading deformation is applied to the vertices prior to the LBS skinning in local coordinates. Because the LBS skinning can introduce a twist, we apply the deformation scaling in the X-Y plane as:

$$\mathbf{p}'_{xy} = \mathbf{p}_{xy}\,\text{Rot}(-\alpha_{\text{twist}}) \begin{pmatrix} 1 & 0 \\ 0 & d \end{pmatrix} \text{Rot}(\alpha_{\text{twist}}),$$

where d is the scale factor calculated as in Figure 5, and α_{twist} is the z-axis rotation part of the LBS matrix.

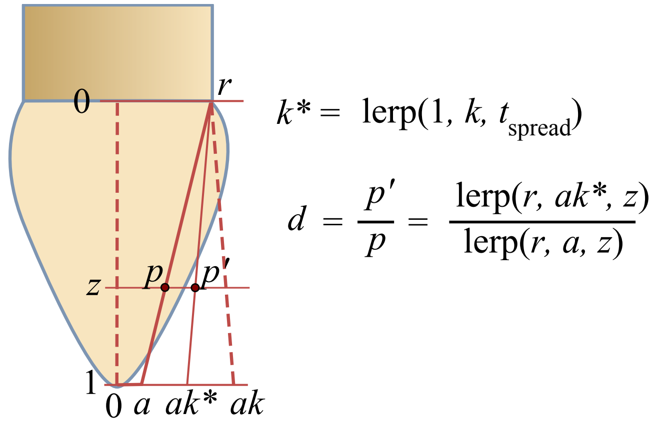

Figure 5: *Implementation of tip spreading on a brush with base half-width r, tip half-width a. k is the maximum spread factor at the tip of the brush, t_{spread} is the fraction of the maximum spread in effect, and k^* is the effective spread factor. z is a normalized coordinate that is 0 at the base of the brush, 1 at the tip. lerp(c_1, c_2, t) is a standard linear interpolation function returning $(1-t)*c_1 + t*c_2$.*

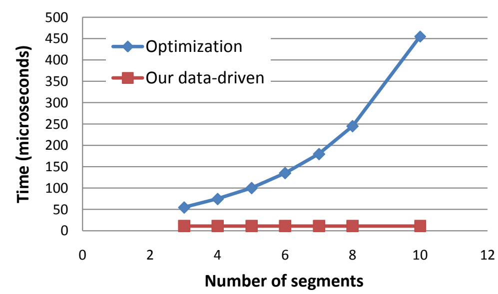

Figure 6: *Time (in microseconds) to calculate control bristle deformations for different numbers of segments using optimization vs. our data-driven method. As the number of segments increases the performance of the optimization method degrades. Performance of our method remains constant.*

4 Experimental results

We have presented a simple and effective technique for simulating the dynamics of brushes via a combination of table-lookup and simplified energy optimization. The result is a simulation technique at least an order of magnitude faster than accurate optimization-based approaches previously presented, and yet it offers more precise deformations based on real-world data.

Figure 6 shows timings comparing performance of our simulation technique vs the optimization technique of [Baxter and Lin 2004], which is a constrained Quasi-Newton SQP method with BFGS Hessian updates, similar also to that of [Chu and Tai 2002]. There is naturally almost no change in simulation cost in our method as the number of segments increases, whereas it rises rapidly with optimization methods like constrained SQP.

Figure 7 demonstrates the impact of brush simulation time on overall paint system performance. In our paint system the simulation update rate is tied to the input device update rate, and in this case it reports at 200 Hz. Points on this horizontal line at 200 Hz represent smooth operation with the paint engine able to keep up with input. In this setup, as the brush update time exceeds 2 msec the impact on performance becomes noticeable. With a simulation time of 2

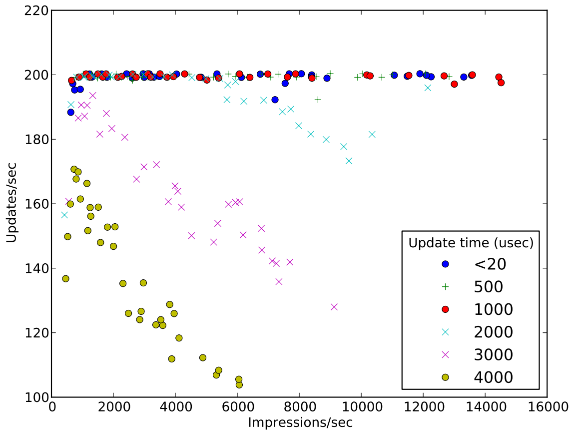

Figure 7: *Impact of brush simulation times on impression rate and update rate. As the time spent on brush simulation updates increases, both maximum impression rate and simulation update rates suffer. 200 Hz is the update rate of the input device (Wacom Intuos3). Test conducted on an Intel Xeon 2.66 GHz CPU, NVIDIA GeForce 8800 GTS 512 GPU.*

msec or more, the system has difficulty keeping up, and the simulation update rate and impression rate both suffer. Such a simulation time could easily be required by an optimization-based brush using 4–8 spines. In contrast, our method will perform acceptably on this system with 1-2 orders of magnitude more spines.

For our system we are using a deformation lookup-table with 15 entries (Figure 3). However in experiments we have found that reasonable results can be had with as few as 6 entries, just using the height minimum and maximum for each of three attack angles. The method does not seem to be particularly sensitive to the number of entries, though six samples do seem to be needed at a minimum. Creating such tables with our manual technique required an hour or two of work, but, again, much of the work could be automated. With a dedicated tool it should only take a few minutes.

Figure 8 shows some typical deformations of the various brushes we have modeled and strokes characteristic of these brushes. The subtle tip deformations give our technique the ability to draw fine lines better than previous optimization approaches. In Figure 9 we show some artwork created using this new brush simulation technique in a painting system similar to that of [Baxter et al. 2001]. Please also see our supplemental video showing the real-time deformations of our brushes.

5 Discussion

Our algorithm has several advantages. It is simple and results in significantly higher performance while modeling complex brush behavior. Moreover, compared to prior physics-based brush modeling methods, our algorithm achieves better numerical stability. As our algorithm is table-driven, it can also be easily implemented on GPUs using vertex shaders.

Nevertheless, our approach does have certain limitations. Since our approach is data-driven, based on a restricted set of "typical" brush deformations, it is not possible to recreate every possible deformation of a real brush. Our approach currently does not incorporate anisotropic friction or brush plasticity, as it simplifies our algorithm. However, our approach is general these things could probably be incorporated.

6 Conclusions and Future Work

In this paper, we presented a simple data-driven algorithm for modeling 3D brushes. Our algorithm uses a small lookup table to efficiently encode the feasible constrained states of a brush. We also model the effects of friction by treating frictional energy as cone-shaped wells centered on the position at the previous time step. In order to model the mesh deformations with higher curvatures, we subdivide the Bézier curves non-uniformly. Our algorithm running on an Intel Xeon 2.66GHz PC is able to simulate brushes with a single spine within 10 microseconds and is 5-45x times faster than optimization-based approaches.

There are many avenues for future work. The general approach of encoding difficult to simulate non-linear constraints in a lookup-table may be useful in other scenarios. Recently shape-matching techniques for simulation have been shown [Müller et al. 2005; Rivers and James 2007] to be effective. These techniques show that dynamics can be simulated if the equilibrium rest shape of an object is known. In that case the deviation between that configuration and the current one can be used to define a position update law for particles that leads to dynamics. Our technique may be extended to define an extended set of rest states based on contact dynamics for an extended class of objects.

Acknowledgments

We would like to thank Craig Mundie, Dan Reed, and John Manferdelli for their support of this work. Also thanks to Nelson Chu who collaborated on the development of the underlying paint system, and to the anonymous artist who painted Figure 9. Finally, our thanks to the anonymous reviewers for their helpful suggestions.

References

ADAMS, B., WICKE, M., DUTRÉ, P., GROSS, M., PAULY, M., AND TESCHNER, M. 2004. Interactive 3D painting on point-sampled objects. *Eurographics Symposium on Point-Based Graphics* (June).

ARTRAGE, 2009. Ambient Design. http://www.artrage.com.

BARAN, I., AND POPOVIĆ, J. 2007. Automatic rigging and animation of 3d characters. *SIGGRAPH '07: ACM SIGGRAPH 2007 papers*, 72.

BAXTER, W. V., AND LIN, M. C. 2004. A versatile interactive 3D brush model. *Proc. of Pacific Graphics 2004*, 319–328.

BAXTER, W., SCHEIB, V., LIN, M., AND MANOCHA, D. 2001. Dab: Haptic painting with 3d virtual brushes. *Proc. of ACM SIGGRAPH*, 461–468.

CHU, N. S., AND TAI, C. L. 2002. An efficient brush model for physically-based 3D painting. *Proc. of Pacific Graphics* (Oct), 413–423.

CORDIER, F., AND MAGNENAT-THALMANN, N. 2004. A data-driven approach for real-time clothes simulation. *Computer Graphics and Applications (Proc. PG 2004)*, 257–266.

GREENE, R. 1985. The drawing prism: a versatile graphic input device. In *Proceedings of the 12th annual conference on Computer graphics and interactive techniques*, ACM Press, 103–110.

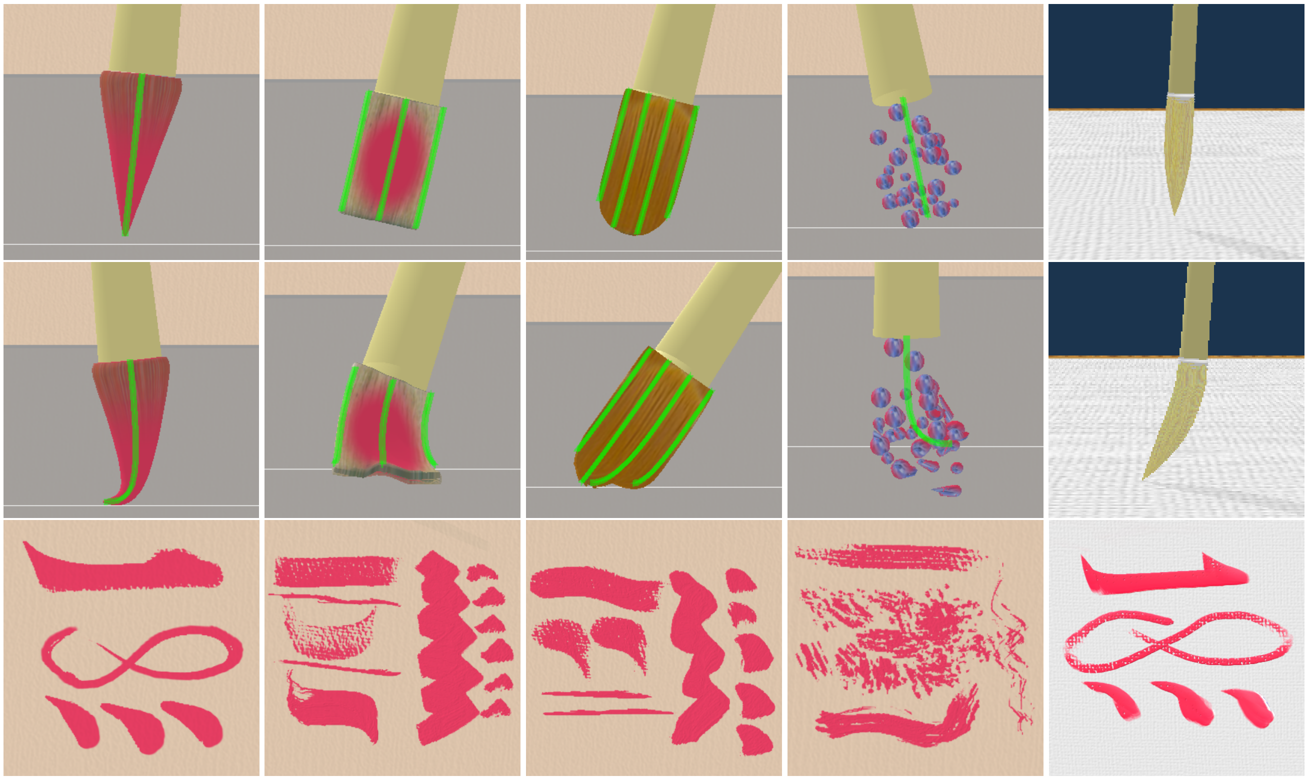

(a) calligraphy (b) flat (c) filbert (d) atypical (e) previous method

Figure 8: *(a)–(d) A variety of our brush models during deformation. (e) Previous optimization-based models often used too few segments for performance reasons, leading to an inability to model subtle tip deformations. Using our technique a single brush can recreate the wide variety of expressive strokes seen in real brushes. Compared with previous optimization-based approaches, our technique can create cleaner and thinner fine lines and has less polygonization with fast strokes due to faster updates.*

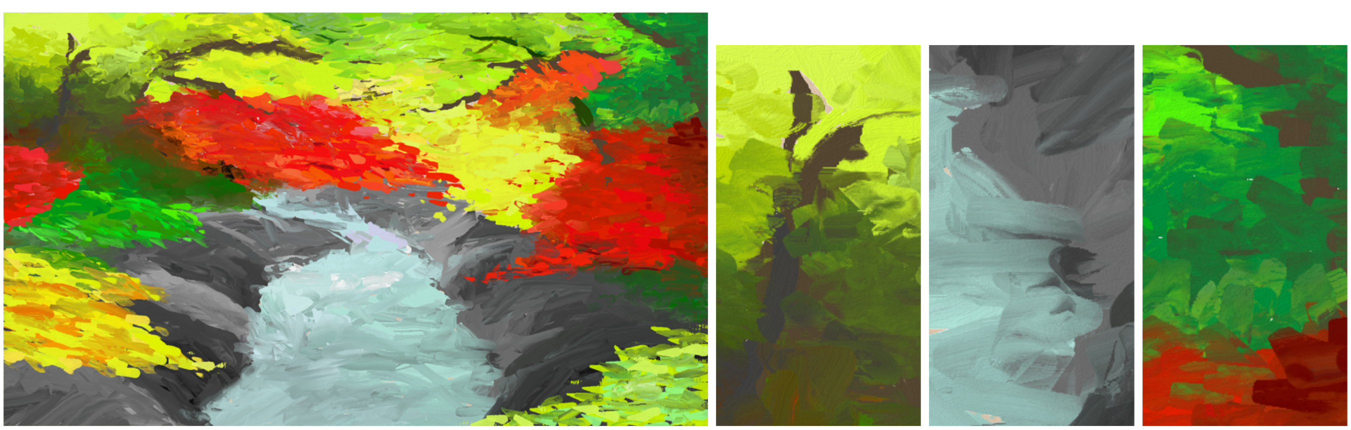

Figure 9: *A painting created by an artist using our new brush model and several details.*

MÜLLER, M., HEIDELBERGER, B., TESCHNER, M., AND GROSS, M. 2005. Meshless deformations based on shape matching. In *SIGGRAPH '05: Proceedings of the 32nd annual conference on Computer graphics and interactive techniques*, 471–478.

PAINTER 11, 2009. Corel.

PHOTOSHOP. 2009. Adobe. *http://www.adobe.com/photoshop/*.

RIVERS, A. R., AND JAMES, D. L. 2007. FastLSM: fast lattice shape matching for robust real-time deformation. *ACM Trans. Graph. 26*, 3, 82.

SAITO, S., AND NAKAJIMA, M. 1999. 3D physically based brush model for painting. *SIGGRAPH99 Conference Abstracts and Applications*, 226.

SMITH, A. R. 1978. Paint. TM 7, NYIT Computer Graphics Lab, July.

STRASSMANN, S. 1986. Hairy brushes. *Computer Graphics (SIGGRAPH'86 Proc.) 20*, 225–232.

VAN LAERHOVEN, T., AND REETH, F. V. 2007. Brush up your painting skills. *The Visual Computer (CGI 2007 special issue) 23*, 9-11, 763–771.

VANDOREN, P., CLAESEN, L., VAN LAERHOVEN, T., TAELMAN, J., AND VAN REETH, F. 2009. FluidPaint: an interactive digital painting system using real wet brushes. In *Proceedings of IEEE Tabletop and Interactive Surfaces*.

WAHBA, G. 1990. *Spline Models for Observational Data*. SIAM.

WHITE, R., CRANE, K., AND FORSYTH, D. A. 2007. Capturing and animating occluded cloth. In *SIGGRAPH '07: ACM SIGGRAPH 2007 papers*, ACM, New York, NY, USA, 34.

WONG, H., AND IP, H. 2000. Virtual brush: A model-based synthesis of chinese calligraphy. *Computers & Graphics 24*.

XU, S., TANG, F., LAU, F., AND PAN, Y. 2002. A solid model based virtual hairy brush. *Computer Graphics Forum (Eurographics '02) 21*, 3, 299–308.

XU, S., LAU, F., TANG, F., AND PAN, Y. 2003. Advanced design for a realistic virtual brush. *Computer Graphics Forum (Eurographics '03) 22*, 3 (September), 533–542.